

## Pair invariant mass to isolate background in the search for the chiral magnetic effect in Au+Au collisions at $\sqrt{s_{NN}} = 200$ GeV

J. Adam,<sup>6</sup> L. Adamczyk,<sup>2</sup> J. R. Adams,<sup>39</sup> J. K. Adkins,<sup>30</sup> G. Agakishiev,<sup>28</sup> M. M. Aggarwal,<sup>41</sup> Z. Ahammed,<sup>61</sup> I. Alekseev,<sup>3,35</sup> D. M. Anderson,<sup>55</sup> A. Aparin,<sup>28</sup> E. C. Aschenauer,<sup>6</sup> M. U. Ashraf,<sup>11</sup> F. G. Atetalla,<sup>29</sup> A. Attri,<sup>41</sup> G. S. Averichev,<sup>28</sup> V. Bairathi,<sup>53</sup> K. Barish,<sup>10</sup> A. Behera,<sup>52</sup> R. Bellwied,<sup>20</sup> A. Bhasin,<sup>27</sup> J. Bielcik,<sup>14</sup> J. Bielcikova,<sup>38</sup> L. C. Bland,<sup>6</sup> I. G. Bordyuzhin,<sup>3</sup> J. D. Brandenburg,<sup>49,6</sup> A. V. Brandin,<sup>35</sup> J. Butterworth,<sup>45</sup> H. Caines,<sup>64</sup> M. Calderón de la Barca Sánchez,<sup>8</sup> D. Cebra,<sup>8</sup> I. Chakaberia,<sup>29,6</sup> P. Chaloupka,<sup>14</sup> B. K. Chan,<sup>9</sup> F-H. Chang,<sup>37</sup> Z. Chang,<sup>6</sup> N. Chankova-Bunzarova,<sup>28</sup> A. Chatterjee,<sup>11</sup> D. Chen,<sup>10</sup> J. H. Chen,<sup>18</sup> X. Chen,<sup>48</sup> Z. Chen,<sup>49</sup> J. Cheng,<sup>57</sup> M. Cherney,<sup>13</sup> M. Chevalier,<sup>10</sup> S. Choudhury,<sup>18</sup> W. Christie,<sup>6</sup> H. J. Crawford,<sup>7</sup> M. Csanád,<sup>16</sup> M. Daugherty,<sup>1</sup> T. G. Dedovich,<sup>28</sup> I. M. Deppner,<sup>19</sup> A. A. Derevschikov,<sup>43</sup> L. Didenko,<sup>6</sup> X. Dong,<sup>31</sup> J. L. Drachenberg,<sup>1</sup> J. C. Dunlop,<sup>6</sup> T. Edmonds,<sup>44</sup> N. Elsey,<sup>63</sup> J. Engelage,<sup>7</sup> G. Eppley,<sup>45</sup> R. Esha,<sup>52</sup> S. Esumi,<sup>58</sup> O. Evdokimov,<sup>12</sup> A. Ewigleben,<sup>32</sup> O. Eyser,<sup>6</sup> R. Fatemi,<sup>30</sup> S. Fazio,<sup>6</sup> P. Federic,<sup>38</sup> J. Fedorisin,<sup>28</sup> C. J. Feng,<sup>37</sup> Y. Feng,<sup>44</sup> P. Filip,<sup>28</sup> E. Finch,<sup>51</sup> Y. Fisyak,<sup>6</sup> A. Francisco,<sup>64</sup> L. Fulek,<sup>2</sup> C. A. Gagliardi,<sup>55</sup> T. Galatyuk,<sup>15</sup> F. Geurts,<sup>45</sup> A. Gibson,<sup>60</sup> K. Gopal,<sup>23</sup> D. Grosnick,<sup>60</sup> W. Guryn,<sup>6</sup> A. I. Hamad,<sup>29</sup> A. Hamed,<sup>5</sup> S. Harabasz,<sup>15</sup> J. W. Harris,<sup>64</sup> S. He,<sup>11</sup> W. He,<sup>18</sup> X. He,<sup>26</sup> S. Heppelmann,<sup>8</sup> S. Heppelmann,<sup>42</sup> N. Herrmann,<sup>19</sup> E. Hoffman,<sup>20</sup> L. Holub,<sup>14</sup> Y. Hong,<sup>31</sup> S. Horvat,<sup>64</sup> Y. Hu,<sup>18</sup> H. Z. Huang,<sup>9</sup> S. L. Huang,<sup>52</sup> T. Huang,<sup>37</sup> X. Huang,<sup>57</sup> T. J. Humanic,<sup>39</sup> P. Huo,<sup>52</sup> G. Igo,<sup>9</sup> D. Isenhower,<sup>1</sup> W. W. Jacobs,<sup>25</sup> C. Jena,<sup>23</sup> A. Jentsch,<sup>6</sup> Y. Ji,<sup>48</sup> J. Jia,<sup>6,52</sup> K. Jiang,<sup>48</sup> S. Jowzaee,<sup>63</sup> X. Ju,<sup>48</sup> E. G. Judd,<sup>7</sup> S. Kabana,<sup>53</sup> M. L. Kabir,<sup>10</sup> S. Kagamaster,<sup>32</sup> D. Kalinkin,<sup>25</sup> K. Kang,<sup>57</sup> D. Kapukchyan,<sup>10</sup> K. Kauder,<sup>6</sup> H. W. Ke,<sup>6</sup> D. Keane,<sup>29</sup> A. Kechechyan,<sup>28</sup> M. Kelsey,<sup>31</sup> Y. V. Khyzhniak,<sup>35</sup> D. P. Kikoła,<sup>62</sup> C. Kim,<sup>10</sup> B. Kimelman,<sup>8</sup> D. Kincses,<sup>16</sup> T. A. Kinghorn,<sup>8</sup> I. Kisel,<sup>17</sup> A. Kiselev,<sup>6</sup> A. Kisiel,<sup>62</sup> M. Kocan,<sup>14</sup> L. Kochenda,<sup>35</sup> L. K. Kosarzewski,<sup>14</sup> L. Kramarik,<sup>14</sup> P. Kravtsov,<sup>35</sup> K. Krueger,<sup>4</sup> N. Kulathunga Mudiyansele,<sup>20</sup> L. Kumar,<sup>41</sup> R. Kunnawalkam Elayavalli,<sup>63</sup> J. H. Kwasizur,<sup>25</sup> R. Lacey,<sup>52</sup> S. Lan,<sup>11</sup> J. M. Landgraf,<sup>6</sup> J. Lauret,<sup>6</sup> A. Lebedev,<sup>6</sup> R. Lednicky,<sup>28</sup> J. H. Lee,<sup>6</sup> Y. H. Leung,<sup>31</sup> C. Li,<sup>48</sup> W. Li,<sup>50</sup> W. Li,<sup>45</sup> X. Li,<sup>48</sup> Y. Li,<sup>57</sup> Y. Liang,<sup>29</sup> R. Licenik,<sup>38</sup> T. Lin,<sup>55</sup> Y. Lin,<sup>11</sup> M. A. Lisa,<sup>39</sup> F. Liu,<sup>11</sup> H. Liu,<sup>25</sup> P. Liu,<sup>52</sup> P. Liu,<sup>50</sup> T. Liu,<sup>64</sup> X. Liu,<sup>39</sup> Y. Liu,<sup>55</sup> Z. Liu,<sup>48</sup> T. Ljubicic,<sup>6</sup> W. J. Llope,<sup>63</sup> R. S. Longacre,<sup>6</sup> N. S. Lukow,<sup>54</sup> S. Luo,<sup>12</sup> X. Luo,<sup>11</sup> G. L. Ma,<sup>50</sup> L. Ma,<sup>18</sup> R. Ma,<sup>6</sup> Y. G. Ma,<sup>50</sup> N. Magdy,<sup>12</sup> R. Majka,<sup>64</sup> D. Mallick,<sup>36</sup> S. Margetis,<sup>29</sup> C. Markert,<sup>56</sup> H. S. Matis,<sup>31</sup> J. A. Mazer,<sup>46</sup> N. G. Minaev,<sup>43</sup> S. Mioduszewski,<sup>55</sup> B. Mohanty,<sup>36</sup> M. M. Mondal,<sup>52</sup> I. Mooney,<sup>63</sup> Z. Moravcova,<sup>14</sup> D. A. Morozov,<sup>43</sup> M. Nagy,<sup>16</sup> J. D. Nam,<sup>54</sup> Md. Nasim,<sup>22</sup> K. Nayak,<sup>11</sup> D. Neff,<sup>9</sup> J. M. Nelson,<sup>7</sup> D. B. Nemes,<sup>64</sup> M. Nie,<sup>49</sup> G. Nigmatkulov,<sup>35</sup> T. Niida,<sup>58</sup> L. V. Nogach,<sup>43</sup> T. Nonaka,<sup>58</sup> G. Odyniec,<sup>31</sup> A. Ogawa,<sup>6</sup> S. Oh,<sup>31</sup> V. A. Okorokov,<sup>35</sup> B. S. Page,<sup>6</sup> R. Pak,<sup>6</sup> A. Pandav,<sup>36</sup> Y. Panebratsev,<sup>28</sup> B. Pawlik,<sup>40</sup> D. Pawlowska,<sup>62</sup> H. Pei,<sup>11</sup> C. Perkins,<sup>7</sup> L. Pinsky,<sup>20</sup> R. L. Pintér,<sup>16</sup> J. Pluta,<sup>62</sup> J. Porter,<sup>31</sup> M. Posik,<sup>54</sup> N. K. Pruthi,<sup>41</sup> M. Przybycien,<sup>2</sup> J. Putschke,<sup>63</sup> H. Qiu,<sup>26</sup> A. Quintero,<sup>54</sup> S. K. Radhakrishnan,<sup>29</sup> S. Ramachandran,<sup>30</sup> R. L. Ray,<sup>56</sup> R. Reed,<sup>32</sup> H. G. Ritter,<sup>31</sup> J. B. Roberts,<sup>45</sup> O. V. Rogachevskiy,<sup>28</sup> J. L. Romero,<sup>8</sup> L. Ruan,<sup>6</sup> J. Rusnak,<sup>38</sup> N. R. Sahoo,<sup>49</sup> H. Sako,<sup>58</sup> S. Salur,<sup>46</sup> J. Sandweiss,<sup>64</sup> S. Sato,<sup>58</sup> W. B. Schmidke,<sup>6</sup> N. Schmitz,<sup>33</sup> B. R. Schweid,<sup>52</sup> F. Seck,<sup>15</sup> J. Seger,<sup>13</sup> M. Sergeeva,<sup>9</sup> R. Seto,<sup>10</sup> P. Seyboth,<sup>33</sup> N. Shah,<sup>24</sup> E. Shahaliev,<sup>28</sup> P. V. Shanmuganathan,<sup>6</sup> M. Shao,<sup>48</sup> F. Shen,<sup>49</sup> W. Q. Shen,<sup>50</sup> S. S. Shi,<sup>11</sup> Q. Y. Shou,<sup>50</sup> E. P. Sichtermann,<sup>31</sup> R. Sikora,<sup>2</sup> M. Simko,<sup>38</sup> J. Singh,<sup>41</sup> S. Singha,<sup>26</sup> N. Smirnov,<sup>64</sup> W. Solyst,<sup>25</sup> P. Sorensen,<sup>6</sup> H. M. Spinka,<sup>4</sup> B. Srivastava,<sup>44</sup> T. D. S. Stanislaus,<sup>60</sup> M. Stefaniak,<sup>62</sup> D. J. Stewart,<sup>64</sup> M. Strikhanov,<sup>35</sup> B. Stringfellow,<sup>44</sup> A. A. P. Suaide,<sup>47</sup> M. Sumner,<sup>38</sup> B. Summa,<sup>42</sup> X. M. Sun,<sup>11</sup> X. Sun,<sup>12</sup> Y. Sun,<sup>48</sup> Y. Sun,<sup>21</sup> B. Surrus,<sup>54</sup> D. N. Svirida,<sup>3</sup> P. Szymanski,<sup>62</sup> A. H. Tang,<sup>6</sup> Z. Tang,<sup>48</sup> A. Taranenko,<sup>35</sup> T. Tarnowsky,<sup>34</sup> J. H. Thomas,<sup>31</sup> A. R. Timmins,<sup>20</sup> D. Tlusty,<sup>13</sup> M. Tokarev,<sup>28</sup> C. A. Tomkiel,<sup>32</sup> S. Trentalange,<sup>9</sup> R. E. Tribble,<sup>55</sup> P. Tribedy,<sup>6</sup> S. K. Tripathy,<sup>16</sup> O. D. Tsai,<sup>9</sup> Z. Tu,<sup>6</sup> T. Ullrich,<sup>6</sup> D. G. Underwood,<sup>4</sup> I. Upsal,<sup>49,6</sup> G. Van Buren,<sup>6</sup> J. Vanek,<sup>38</sup> A. N. Vasiliev,<sup>43</sup> I. Vassiliev,<sup>17</sup> F. Videbæk,<sup>6</sup> S. Vokal,<sup>28</sup> S. A. Voloshin,<sup>63</sup> F. Wang,<sup>44</sup> G. Wang,<sup>9</sup> J. S. Wang,<sup>21</sup> P. Wang,<sup>48</sup> Y. Wang,<sup>11</sup> Y. Wang,<sup>57</sup> Z. Wang,<sup>49</sup> J. C. Webb,<sup>6</sup> P. C. Weidenkaff,<sup>19</sup> L. Wen,<sup>9</sup> G. D. Westfall,<sup>34</sup> H. Wieman,<sup>31</sup> S. W. Wissink,<sup>25</sup> R. Witt,<sup>59</sup> Y. Wu,<sup>10</sup> Z. G. Xiao,<sup>57</sup> G. Xie,<sup>31</sup> W. Xie,<sup>44</sup> H. Xu,<sup>21</sup> N. Xu,<sup>31</sup> Q. H. Xu,<sup>49</sup> Y. F. Xu,<sup>50</sup> Y. Xu,<sup>49</sup> Z. Xu,<sup>6</sup> Z. Xu,<sup>9</sup> C. Yang,<sup>49</sup> Q. Yang,<sup>49</sup> S. Yang,<sup>6</sup> Y. Yang,<sup>37</sup> Z. Yang,<sup>11</sup> Z. Ye,<sup>45</sup> Z. Ye,<sup>12</sup> L. Yi,<sup>49</sup> K. Yip,<sup>6</sup> H. Zbroszczyk,<sup>62</sup> W. Zha,<sup>48</sup> D. Zhang,<sup>11</sup> S. Zhang,<sup>48</sup> S. Zhang,<sup>50</sup> X. P. Zhang,<sup>57</sup> Y. Zhang,<sup>48</sup> Y. Zhang,<sup>11</sup> Z. J. Zhang,<sup>37</sup> Z. Zhang,<sup>6</sup> Z. Zhang,<sup>12</sup> J. Zhao,<sup>44</sup> C. Zhong,<sup>50</sup> C. Zhou,<sup>50</sup> X. Zhu,<sup>57</sup> Z. Zhu,<sup>49</sup> M. Zurek,<sup>31</sup> and M. Zyzak<sup>17</sup>

(STAR Collaboration)

- <sup>2</sup>AGH University of Science and Technology, FPACS, Cracow 30-059, Poland
- <sup>3</sup>Alikhanov Institute for Theoretical and Experimental Physics NRC "Kurchatov Institute", Moscow 117218, Russia
- <sup>4</sup>Argonne National Laboratory, Argonne, Illinois 60439
- <sup>5</sup>American University of Cairo, New Cairo 11835, New Cairo, Egypt
- <sup>6</sup>Brookhaven National Laboratory, Upton, New York 11973
- <sup>7</sup>University of California, Berkeley, California 94720
- <sup>8</sup>University of California, Davis, California 95616
- <sup>9</sup>University of California, Los Angeles, California 90095
- <sup>10</sup>University of California, Riverside, California 92521
- <sup>11</sup>Central China Normal University, Wuhan, Hubei 430079
- <sup>12</sup>University of Illinois at Chicago, Chicago, Illinois 60607
- <sup>13</sup>Creighton University, Omaha, Nebraska 68178
- <sup>14</sup>Czech Technical University in Prague, FNSPE, Prague 115 19, Czech Republic
- <sup>15</sup>Technische Universität Darmstadt, Darmstadt 64289, Germany
- <sup>16</sup>ELTE Eötvös Loránd University, Budapest, Hungary H-1117
- <sup>17</sup>Frankfurt Institute for Advanced Studies FIAS, Frankfurt 60438, Germany
- <sup>18</sup>Fudan University, Shanghai, 200433
- <sup>19</sup>University of Heidelberg, Heidelberg 69120, Germany
- <sup>20</sup>University of Houston, Houston, Texas 77204
- <sup>21</sup>Huzhou University, Huzhou, Zhejiang 313000
- <sup>22</sup>Indian Institute of Science Education and Research (IISER), Berhampur 760010, India
- <sup>23</sup>Indian Institute of Science Education and Research (IISER) Tirupati, Tirupati 517507, India
- <sup>24</sup>Indian Institute Technology, Patna, Bihar 801106, India
- <sup>25</sup>Indiana University, Bloomington, Indiana 47408
- <sup>26</sup>Institute of Modern Physics, Chinese Academy of Sciences, Lanzhou, Gansu 730000
- <sup>27</sup>University of Jammu, Jammu 180001, India
- <sup>28</sup>Joint Institute for Nuclear Research, Dubna 141 980, Russia
- <sup>29</sup>Kent State University, Kent, Ohio 44242
- <sup>30</sup>University of Kentucky, Lexington, Kentucky 40506-0055
- <sup>31</sup>Lawrence Berkeley National Laboratory, Berkeley, California 94720
- <sup>32</sup>Lehigh University, Bethlehem, Pennsylvania 18015
- <sup>33</sup>Max-Planck-Institut für Physik, Munich 80805, Germany
- <sup>34</sup>Michigan State University, East Lansing, Michigan 48824
- <sup>35</sup>National Research Nuclear University MEPhI, Moscow 115409, Russia
- <sup>36</sup>National Institute of Science Education and Research, HBNI, Jatni 752050, India
- <sup>37</sup>National Cheng Kung University, Tainan 70101
- <sup>38</sup>Nuclear Physics Institute of the CAS, Rez 250 68, Czech Republic
- <sup>39</sup>Ohio State University, Columbus, Ohio 43210
- <sup>40</sup>Institute of Nuclear Physics PAN, Cracow 31-342, Poland
- <sup>41</sup>Panjab University, Chandigarh 160014, India
- <sup>42</sup>Pennsylvania State University, University Park, Pennsylvania 16802
- <sup>43</sup>NRC "Kurchatov Institute", Institute of High Energy Physics, Protvino 142281, Russia
- <sup>44</sup>Purdue University, West Lafayette, Indiana 47907
- <sup>45</sup>Rice University, Houston, Texas 77251
- <sup>46</sup>Rutgers University, Piscataway, New Jersey 08854
- <sup>47</sup>Universidade de São Paulo, São Paulo, Brazil 05314-970
- <sup>48</sup>University of Science and Technology of China, Hefei, Anhui 230026
- <sup>49</sup>Shandong University, Qingdao, Shandong 266237
- <sup>50</sup>Shanghai Institute of Applied Physics, Chinese Academy of Sciences, Shanghai 201800
- <sup>51</sup>Southern Connecticut State University, New Haven, Connecticut 06515
- <sup>52</sup>State University of New York, Stony Brook, New York 11794
- <sup>53</sup>Instituto de Alta Investigación, Universidad de Tarapacá, Chile
- <sup>54</sup>Temple University, Philadelphia, Pennsylvania 19122
- <sup>55</sup>Texas A&M University, College Station, Texas 77843
- <sup>56</sup>University of Texas, Austin, Texas 78712
- <sup>57</sup>Tsinghua University, Beijing 100084
- <sup>58</sup>University of Tsukuba, Tsukuba, Ibaraki 305-8571, Japan
- <sup>59</sup>United States Naval Academy, Annapolis, Maryland 21402
- <sup>60</sup>Valparaiso University, Valparaiso, Indiana 46383
- <sup>61</sup>Variable Energy Cyclotron Centre, Kolkata 700064, India
- <sup>62</sup>Warsaw University of Technology, Warsaw 00-661, Poland
- <sup>63</sup>Wayne State University, Detroit, Michigan 48201
- <sup>64</sup>Yale University, New Haven, Connecticut 06520

(Dated: April 2, 2021)

Quark interactions with topological gluon configurations can induce local chirality imbalance and parity violation in quantum chromodynamics, which can lead to the chiral magnetic effect (CME) – an electric charge separation along the strong magnetic field in relativistic heavy-ion collisions. The CME-sensitive azimuthal correlator observable ( $\Delta\gamma$ ) is contaminated by background arising, in part, from resonance decays coupled with elliptic anisotropy ( $v_2$ ). We report here the first differential measurements of the correlator as a function of the pair invariant mass ( $m_{\text{inv}}$ ) in 20-50% centrality Au+Au collisions at  $\sqrt{s_{\text{NN}}}$  = 200 GeV by the STAR experiment at RHIC. Strong resonance background contributions to  $\Delta\gamma$  are observed. At large  $m_{\text{inv}}$  where this background is significantly reduced, the  $\Delta\gamma$  value is found to be also significantly smaller. An event shape engineering technique is deployed to determine the  $v_2$  background shape as a function of  $m_{\text{inv}}$ . A  $v_2$ -independent signal, possibly indicating a  $m_{\text{inv}}$ -integrated CME contribution, is extracted to be  $\Delta\gamma_{\text{signal}} = (0.03 \pm 0.06 \pm 0.08) \times 10^{-4}$ , or  $(2 \pm 4 \pm 5)\%$  of the inclusive  $\Delta\gamma(m_{\text{inv}} > 0.4 \text{ GeV}/c^2) = (1.58 \pm 0.02 \pm 0.02) \times 10^{-4}$ . This presents an upper limit of  $0.23 \times 10^{-4}$ , or 15% of the inclusive result at 95% confidence level.

PACS numbers: 25.75.-q, 25.75.Gz, 25.75.Ld

Quark interactions with a fluctuating topological gluon field can induce chirality imbalance and local parity violation in quantum chromodynamics (QCD) [1–3]. This can lead to electric charge separation in the presence of a strong magnetic field ( $\vec{B}$ ), a phenomenon known as the chiral magnetic effect (CME) [4, 5]. Such a strong  $\vec{B}$  may be present in non-central heavy-ion collisions, mainly generated by the spectator protons at early times [6, 7]. Extensive theoretical and experimental efforts have been devoted to the search for the CME-induced charge separation along  $\vec{B}$  in heavy-ion collisions [8–10].

In non-central heavy-ion collisions, the second-order harmonic plane of the spatial distribution of the participant nucleons (participant plane) [11], although fluctuating, is generally aligned with the reaction plane (defined by the impact parameter direction and the beam), thus generally perpendicular to  $\vec{B}$  on average. The participant plane can be assessed by the second-order harmonic plane ( $\psi_2$ ) from final-state particle azimuthal distributions. The commonly used observable to measure the charge separation is the three-point correlator with respect to  $\psi_2$  [12]:

$$\gamma \equiv \cos(\phi_\alpha + \phi_\beta - 2\psi_2), \quad (1)$$

where  $\phi_\alpha$  and  $\phi_\beta$  are the azimuthal angles of particles  $\alpha$  and  $\beta$ , respectively. Because of the charge-independent correlation background (e.g. from global momentum conservation), often the correlator difference is used [12],  $\Delta\gamma \equiv \gamma_{\text{OS}} - \gamma_{\text{SS}}$ , where  $\gamma_{\text{OS}}$  stands for the  $\gamma$  of opposite-sign pairs ( $\alpha$  and  $\beta$  have the opposite-sign electric charges) and  $\gamma_{\text{SS}}$  for that of same-sign pairs ( $\alpha$  and  $\beta$  have the same-sign electric charge).

Significant  $\Delta\gamma$  is indeed observed in heavy-ion collisions on the order of  $10^{-4}$  in mid-central collisions [13–17]. A difficulty in its interpretation as originating from the CME-induced charge separation is the large charge-dependent background contributions to  $\Delta\gamma$  [10, 17–22], such as those from resonance decays [12, 23]. This is because the  $\Delta\gamma$  variable is ambiguous between a CME-induced back-to-back OS pair perpendicular to  $\psi_2$  (charge separation) and an OS pair from a resonance de-

cay along  $\psi_2$  (charge conservation). There are more particles/resonances produced along the  $\psi_2$  than perpendicular, the relative difference of which is quantified by the elliptic flow anisotropy parameter  $v_{2,\text{res}}$ . The background arises from the coupling of this flow anisotropy, and the intrinsic decay correlation (nonflow) can be expressed as:

$$\Delta\gamma_{\text{bkgd}} \propto \langle \cos(\phi_\alpha + \phi_\beta - 2\phi_{\text{res}}) \rangle v_{2,\text{res}}, \quad (2)$$

where  $\phi_{\text{res}}$  is the azimuthal angle of the resonance, and  $\alpha$  and  $\beta$  are the resonance decay daughters [10, 12, 20, 23, 24]. Early model studies [13, 14] indicated that the background contributions were unable to fully account for the measured  $\Delta\gamma$ . It was pointed out recently that one of the reasons was an insufficient description of the  $v_2$  anisotropy by the models [25]. Such background sources are amply demonstrated by small-system collisions, where the participant plane is determined purely by geometry fluctuations, essentially uncorrelated with the impact parameter or the  $\vec{B}$  direction [17]. Therefore any CME signal is expected to be negligible in small systems. However, a large  $\Delta\gamma$  signal was observed in  $p$ +Pb collisions at the LHC, similar to that in Pb+Pb collisions. This challenged the CME interpretation of the heavy-ion data [17]. A large  $\Delta\gamma$  signal is also observed in  $p(d)$ +Au collisions at RHIC [26].

In order to isolate the resonance background contributions, we report new measurements of the  $\Delta\gamma$  variable, differential in pair invariant mass ( $m_{\text{inv}}$ ). The integral  $\Delta\gamma$  with a minimum  $m_{\text{inv}}$  limit is presented. To fully exploit the data, an event shape engineering (ESE) [27] technique is deployed where events with different  $v_2$  but same CME signal are selected so to determine the  $v_2$  background shape as a function of  $m_{\text{inv}}$ . The  $\Delta\gamma(m_{\text{inv}})$  data are then fitted to the  $v_2$  background shape plus a  $m_{\text{inv}}$ -independent constant term. The extracted constant term represents a  $v_2$ -independent component in the data, possibly a  $m_{\text{inv}}$ -integrated CME signal.

The data reported here were taken by the STAR experiment at the center-of-mass energy per nucleon pair of  $\sqrt{s_{\text{NN}}} = 200$  GeV in the year 2011, 2014 and 2016. A total of 2.5 billions minimum-bias (MB) triggered events

were used in the analysis. The STAR apparatus is described in Ref. [28].

The main detectors used in this analysis are the time projection chamber (TPC) [29, 30] and the time-of-flight (TOF) detector [31]. Track trajectories are reconstructed from hits detected in the TPC; at least 10 points out of a possible maximum of 45 points are required for a valid track. The primary interaction vertex is reconstructed from charged particle tracks. The event centrality is determined from charged particle multiplicity for tracks which are within pseudorapidity  $|\eta| < 0.5$ , and have distance of closest approach (DCA) to the primary vertex of less than 3 cm. Events with primary vertices within 30 cm (year 2011) or 6 cm (years 2014, 2016) longitudinally and within 2 cm in the transverse plane from the geometrical center of the TPC are used.

Tracks used for the analysis are required to have at least 20 points, and to have DCA less than 1 cm. The fraction of points used to reconstruct a track out of the maximum number of points allowed for the track by the TPC geometry is required to be greater than 0.52 to avoid track splitting. Particle momenta are determined by the track trajectories in the STAR magnetic field. A minimum transverse momentum ( $p_T > 0.2$  GeV/ $c$ ) is required to ensure that each charged track traveling through the TPC can reach the TOF detector inside the STAR magnet. The charged particles can be identified by measuring their ionization energy loss ( $dE/dx$ ) in the TPC gas and their time of flight using the TOF detector. Pions are identified up to  $p_T = 0.8$  GeV/ $c$  with TPC  $dE/dx$  information, and extended to  $p_T = 1.8$  GeV/ $c$  with the TOF.

This analysis uses the three-particle correlator method to define  $\gamma$ :

$$\gamma = \langle \cos(\phi_\alpha + \phi_\beta - 2\phi_c) \rangle / v_{2,c}, \quad (3)$$

where  $\alpha$  and  $\beta$  represent the pion index, and the average  $\langle \dots \rangle$  runs over all triplets and over all events. The azimuthal angle of the third particle,  $\phi_c$ , serves as a measure of  $\psi_2$ . The imprecision in determining the  $\psi_2$  by a single particle is corrected by dividing by the resolution factor, equal to the particle's elliptic flow anisotropy  $v_{2,c}$ . Charged TPC tracks with  $p_T$  from 0.2 to 2 GeV/ $c$  are used for particle  $c$ . Two methods are used: 1) sub-event method, the main method used in this analysis, where the  $\alpha$ ,  $\beta$  particles are from one half of the TPC ( $-1 < \eta < -0.05$  or  $0.05 < \eta < 1$ ) and the particle  $c$  is from the other half of the TPC ( $0.05 < \eta < 1$  or  $-1 < \eta < -0.05$ ) [32]; 2) full-event method, where the  $\alpha$ ,  $\beta$  and  $c$  particle are all taken from the pseudo-rapidity range  $|\eta| < 1$  [13, 14]. In order to identify resonance decay contributions, the  $\Delta\gamma$  correlator is studied as a function of  $m_{\text{inv}}$  of the  $\alpha$  and  $\beta$  particle pairs. The analysis loops over  $\alpha$  and  $\beta$  particles, and the  $c$  particle is handled by the cumulant method [33].

The systematic uncertainties are estimated for each run by varying the required minimum number of points

from 20 to 15, and the DCA of the track from 1.0 cm to 2.0 and 0.8 cm. In the full-event method, the  $\eta$  gap used to determine  $v_{2,c}$  via two-particle correlations is varied from 1 to 0.5 and 1.4 [26, 32]. In the sub-event method, the  $\eta$  gap between the east and west sub-events is varied from 0.1 to 0.3 [34]. In the systematic uncertainty estimation of each source, the statistical fluctuation effect arising from the change in the data sample due to each variation is subtracted. For each source when multiple variations are assessed, the systematic uncertainty is taken as the root mean square. The systematic uncertainties from the above sources are added in quadrature for each dataset of the three runs. The three datasets are then combined assuming their systematic uncertainties are fully correlated. The final value is quoted as  $\pm 1$  standard deviation of the systematic uncertainty and as functions of  $m_{\text{inv}}$ . For the extracted possible CME signal from the ESE fit method, a fit result is obtained for each of the above variations, and the systematic uncertainty is estimated in the same way as described above. The  $m_{\text{inv}}$  range used to extract the possible signal is varied from above 0.4 GeV/ $c^2$  to above 0.35 and 0.45 GeV/ $c^2$ , which yields negligible change in the results. Table I lists the total systematic uncertainty and the individual contributions on the extracted possible CME signal relative to the inclusive  $\Delta\gamma$  from the ESE fit method.

| total     | dca       | nHits     | sub-event $\eta$ gap |
|-----------|-----------|-----------|----------------------|
| $\pm 5\%$ | $\pm 2\%$ | $\pm 3\%$ | $\pm 3\%$            |

TABLE I. The absolute systematic uncertainties on the extracted possible CME signal (expressed in percentage) in terms of the inclusive  $\Delta\gamma$  in 20-50% centrality Au+Au collisions at 200 GeV from the ESE fit method.

Figure 1 (a) shows the relative OS and SS  $\pi$ - $\pi$  pair abundance difference,  $r = (N_{OS} - N_{SS})/N_{OS}$ , as a function of  $m_{\text{inv}}$  for 20-50% centrality Au+Au collisions at  $\sqrt{s_{\text{NN}}} = 200$  GeV. Figure 1 (b) shows the measured  $\Delta\gamma$  as a function of  $m_{\text{inv}}$  in a similar way. The sub-event method is used. The  $m_{\text{inv}} < 0.4$  GeV/ $c^2$  region is excluded because the acceptance difference between OS and SS pairs, mostly close in azimuthal angle, starts to become severe. A clear peak from  $K_s^0 \rightarrow \pi^+ + \pi^-$  decay is observed in  $\Delta\gamma$ , and possible  $\rho^0$  and  $f^0$  peaks are also visible [35]. These peaks correspond to the resonance production peaks in  $r$  shown in panel (a) of Fig. 1. The results indicate strong contributions from resonances to the  $\Delta\gamma$  observable.

As indicated by Fig. 1 (a), most of the excess of OS over SS pion pair contributions are from the small  $m_{\text{inv}}$  region. Applying a minimum  $m_{\text{inv}}$  requirement would reduce those contributions. It may, however, also reduce the possible CME signal, likely decreasing with the pion  $p_T$  [6, 13] ( $\langle p_T \rangle \sim m_{\text{inv}}/2$ ), though a recent study [36] suggests a rather  $p_T$  independent signal above 0.2 GeV/ $c$ . Nevertheless, it is interesting to examine

the  $\Delta\gamma(m_{\text{inv}} > m_{\text{inv}}^{\text{low}})$  above a certain  $m_{\text{inv}}^{\text{low}}$  value, which would be more sensitive to the CME signal if the signal is a more slowly decreasing function of  $m_{\text{inv}}$  than resonance contributions. This is shown in Fig. 2 where the full-event method is used. The  $\Delta\gamma(m_{\text{inv}} > m_{\text{inv}}^{\text{low}})$  decreases with increasing  $m_{\text{inv}}^{\text{low}}$  and approaches zero when  $m_{\text{inv}}^{\text{low}}$  becomes large. Note that residual resonance and other correlation backgrounds may still remain at high mass, and detailed model and theoretical studies are required to draw further conclusions.

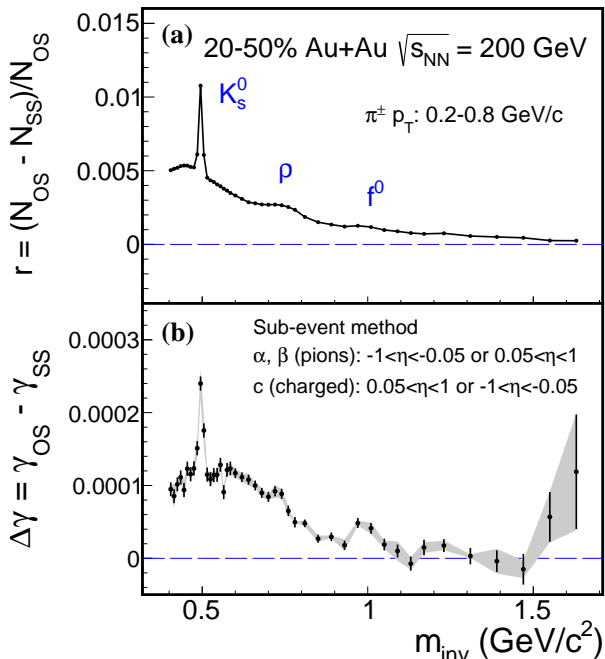


FIG. 1. Pion pair invariant mass ( $m_{\text{inv}}$ ) dependences of (a) the relative excess of opposite-sign (OS) over same-sign (SS) pion pairs,  $r = (N_{\text{OS}} - N_{\text{SS}})/N_{\text{OS}}$ , and (b) the three-point correlator difference,  $\Delta\gamma = \gamma_{\text{OS}} - \gamma_{\text{SS}}$  in 20-50% centrality Au+Au collisions at 200 GeV. The pions are identified by TPC  $dE/dx$  up to  $p_T = 0.8$  GeV/c. The  $\alpha, \beta$  particles (pions) are from one half of the TPC and the particle  $c$  (unidentified charged particle) is from the other half. Error bars are statistical errors. The shaded areas (b) are systematic uncertainties.

In order to fully exploit the data to extract a possible CME signal over the entire  $m_{\text{inv}}$  range, resonance contributions need to be removed. This may be achieved by taking advantage of the presumably different  $m_{\text{inv}}$  dependences of the background and the possible CME signal. Assuming the  $\Delta\gamma$  data contain two-components of a possible  $v_2$ -independent signal and the  $v_2$ -dependent background, the inclusive  $\Delta\gamma$  can be expressed as [37]

$$\Delta\gamma(m_{\text{inv}}) = r(m_{\text{inv}})\langle\cos(\phi_\alpha + \phi_\beta - 2\phi_{\text{res.}})\rangle v_{2,\text{res.}} + \Delta\gamma_{\text{signal}}. \quad (4)$$

The  $v_2$ -independent component may represent the possible CME signal,  $\Delta\gamma_{\text{signal}}$ . The  $m_{\text{inv}}$  shape of the back-

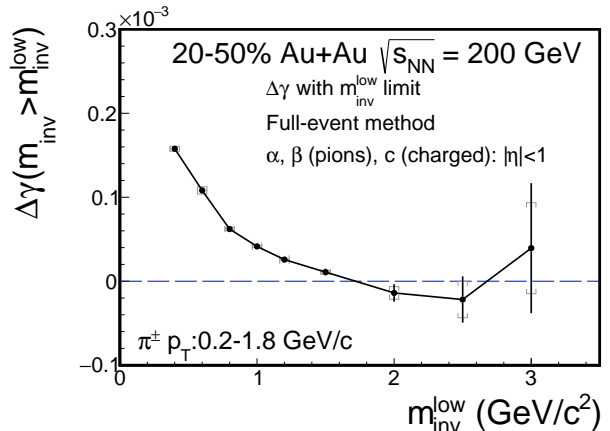


FIG. 2. The identified  $\pi$  pair  $\Delta\gamma$  at  $m_{\text{inv}} > m_{\text{inv}}^{\text{low}}$  as a function of  $m_{\text{inv}}^{\text{low}}$ . The pions are identified by TPC  $dE/dx$  and TOF up to  $p_T = 1.8$  GeV/c. All three particles ( $\alpha, \beta, c$ ) are from the full TPC acceptance ( $|\eta| < 1$ ). Error bars are statistical errors. The grey caps are systematic uncertainties.

ground, the first term of Eq. 4 on the right hand side, can be assessed by the ESE method, selecting events from a narrow centrality bin with different  $v_2$  values by using the reduced flow vector  $q_2$  quantity;  $q_2 = |\sum_{j=1}^N e^{i2\phi_j}|/\sqrt{N}$  summing over the  $\alpha, \beta$  particles in each event. The difference of the  $\Delta\gamma(m_{\text{inv}})$  from the different  $q_2$  classes can be regarded as the background  $\Delta\gamma(m_{\text{inv}})$  shape [9], because the CME for events within a narrow centrality bin are the same even for different  $q_2$  classes (the spectator protons and the participant particle anisotropy are uncorrelated [38]). We have verified that the  $r(m_{\text{inv}})$  distributions are the same between the two event classes, and the decay angular correlations are presumably also the same. Since the  $\alpha, \beta$  particles are used for  $q_2$  calculation, this ESE method is selecting mainly on the statistical fluctuations of the  $\alpha/\beta$  particle's elliptic anisotropy.

The events shown in Fig. 1 are divided into two equal-size groups according to the  $q_2$  value: event sample A with the 50% largest  $q_2$  and event sample B with the 50% smallest  $q_2$ . Figure 3 (a) shows the  $m_{\text{inv}}$  dependence of the  $\Delta\gamma_A$  and  $\Delta\gamma_B$  from ESE-selected event samples A and B, respectively, integrated over the 20-50% centrality range. Figure 3 (b) shows the inclusive (no  $q_2$  restriction, i.e. the same data as shown in Fig. 1 (b))  $\Delta\gamma$  compared with  $\Delta\gamma_A - \Delta\gamma_B$ . The systematic uncertainty of the latter is larger than twice that of the former, which is approximately  $(\Delta\gamma_A + \Delta\gamma_B)/2$ . This is due to an anticorrelation between the two event classes as they are selected largely on statistical fluctuations as aforementioned.

The inclusive  $\Delta\gamma$  contains both the background and the possible CME. With the background shape given by  $\Delta\gamma_A - \Delta\gamma_B$ , the possible CME signal can be extracted from a two component fit:  $\Delta\gamma = b(\Delta\gamma_A - \Delta\gamma_B) + \Delta\gamma_{\text{signal}}$ , assuming  $\Delta\gamma_{\text{signal}}$  is independent of  $m_{\text{inv}}$ . However, since

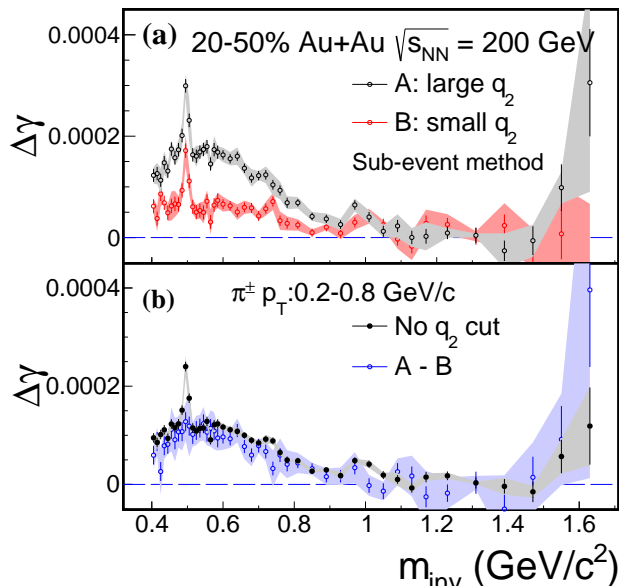


FIG. 3. Pion pair invariant mass ( $m_{\text{inv}}$ ) dependences of (a) the  $\Delta\gamma$  from ESE-selected event samples A (50% largest  $q_2$ ) and B (50% smallest  $q_2$ ), respectively, and (b) the inclusive (no  $q_2$  restriction)  $\Delta\gamma$  compared with  $\Delta\gamma_A - \Delta\gamma_B$  in 20-50% centrality Au+Au collisions at 200 GeV. The pions are identified by TPC  $dE/dx$  up to  $p_T = 0.8$  GeV/c. The  $\alpha$ ,  $\beta$  particles (pions) are from one half of the TPC and the particle  $c$  (unidentified charged particle) is from the other half. Error bars are statistical errors. The shaded areas are systematic uncertainties.

the same data are used in  $\Delta\gamma$  and  $\Delta\gamma_A - \Delta\gamma_B$ , their statistical errors are not independent. To properly handle statistical errors, an alternative function is used to fit the two independent measurements of  $\Delta\gamma_A$  versus  $\Delta\gamma_B$ , namely:

$$\Delta\gamma_B = k\Delta\gamma_A + (1 - k)\Delta\gamma_{\text{signal}}, \quad (5)$$

where  $k$  and  $\Delta\gamma_{\text{signal}}$  are the fit parameters. If  $\Delta\gamma = (\Delta\gamma_A + \Delta\gamma_B)/2$ , then  $b = (1 + k)/(1 - k)/2$ . In this fit model, the background is not required to be strictly proportional to  $v_2$  [37, 39]. Figure 4 shows  $\Delta\gamma_A$  versus  $\Delta\gamma_B$  in 20-50% centrality Au+Au collisions at 200 GeV. Each data point corresponds to one  $m_{\text{inv}}$  bin in Fig. 3 (a). The line is the fits by Eq. 5. The good  $\chi^2/\text{ndf}$  indicates that the fit model assumption of a  $m_{\text{inv}}$ -independent  $\Delta\gamma_{\text{signal}}$  is reasonable. The potential CME is likely dependent of  $m_{\text{inv}}$ , the feature of which could in principle, given enough statistics, be revealed experimentally by more sophisticated ESE analysis. The fitted  $\Delta\gamma_{\text{signal}}$  is  $(0.03 \pm 0.06 \pm 0.08) \times 10^{-4}$  and is found to be  $(2 \pm 4 \pm 5) \%$  of the inclusive  $\Delta\gamma(m_{\text{inv}} > 0.4 \text{ GeV}/c^2) = (1.58 \pm 0.02 \pm 0.02) \times 10^{-4}$ . These values represent over an order of magnitude reduction from the inclusive  $\Delta\gamma$  measurement. Our results indicate that the possible CME signal is small in the inclusive  $\Delta\gamma$ , consistent with zero with current precision. This presents an

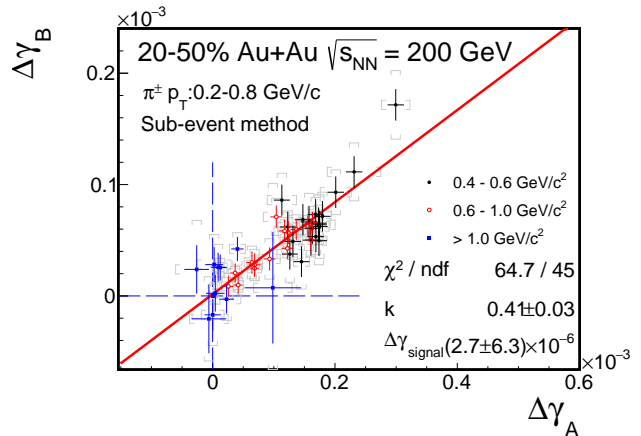


FIG. 4.  $\Delta\gamma_A$  versus  $\Delta\gamma_B$  in 20-50% centrality Au+Au collisions at 200 GeV, superimposed on the linear function fit of Eq. 5. Error bars are statistical errors. Horizontal and vertical caps are the systematic uncertainties on  $\Delta\gamma_A$  and  $\Delta\gamma_B$ , respectively. Different colors indicate the data from different  $m_{\text{inv}}$  regions (black points: 0.4-0.6 GeV/c<sup>2</sup>, red points: 0.6-1.0 GeV/c<sup>2</sup>, blue points: > 1.0 GeV/c<sup>2</sup>).

upper limit of  $0.23 \times 10^{-4}$ , or 15% of the inclusive result at 95% confidence level [40].

In summary, we report differential measurements of the reaction-plane-dependent azimuthal correlation of pion pairs ( $\Delta\gamma$ ), sensitive to the topological-charge-induced chiral magnetic effect (CME) in QCD, as a function of the pair invariant mass ( $m_{\text{inv}}$ ). Resonance structures are observed in  $\Delta\gamma(m_{\text{inv}})$ , indicating major background contributions. At large  $m_{\text{inv}}$ , where this background is significantly reduced, the  $\Delta\gamma$  is also significantly smaller. To isolate the possible CME signal from background, event shape engineering by the sub-event method is used to determine the background shape in  $m_{\text{inv}}$ . The background shape is used in a two-component fit to the  $\Delta\gamma(m_{\text{inv}})$  data, assuming it contains a  $v_2$ -independent signal in addition to the  $v_2$ -dependent background. Such a fit yields a  $v_2$ -independent signal of  $\Delta\gamma_{\text{signal}} = (0.03 \pm 0.06 \pm 0.08) \times 10^{-4}$  in 20-50% centrality Au+Au collisions at 200 GeV,  $(2 \pm 4 \pm 5)\%$  of the inclusive measurement of  $\Delta\gamma(m_{\text{inv}} > 0.4 \text{ GeV}/c^2) = (1.58 \pm 0.02 \pm 0.02) \times 10^{-4}$ , within pion  $p_T = 0.2 - 0.8$  GeV/c and averaged between pseudorapidity ranges of  $-1 < \eta < -0.05$  and  $0.05 < \eta < 1$ . This may represent a possible CME signal integrated over  $m_{\text{inv}}$ , an upper limit of  $0.23 \times 10^{-4}$ , or 15% of the inclusive result at 95% confidence level.

We thank the RHIC Operations Group and RCF at BNL, the NERSC Center at LBNL, and the Open Science Grid consortium for providing resources and support. This work was supported in part by the Office of Nuclear Physics within the U.S. DOE Office of Science, the U.S. National Science Foundation, the Ministry of Education and Science of the Russian Federation, National Natural Science Foundation of China, Chi-

nese Academy of Science, the Ministry of Science and Technology of China and the Chinese Ministry of Education, the Higher Education Sprout Project by Ministry of Education at NCKU, the National Research Foundation of Korea, Czech Science Foundation and Ministry of Education, Youth and Sports of the Czech Republic, Hungarian National Research, Development and Innovation Office, New National Excellency Programme of the Hungarian Ministry of Human Capacities, Department of Atomic Energy and Department of Science and Technology of the Government of India, the National Science Centre of Poland, the Ministry of Science, Education and Sports of the Republic of Croatia, RosAtom of Russia and German Bundesministerium für Bildung, Wissenschaft, Forschung und Technologie (BMBF), Helmholtz Association, Ministry of Education, Culture, Sports, Science, and Technology (MEXT) and Japan Society for the Promotion of Science (JSPS).

- 
- [1] T. D. Lee and G. C. Wick. Vacuum Stability and Vacuum Excitation in a Spin 0 Field Theory. *Phys. Rev. D*, 9:2291–2316, 1974.
- [2] Dmitri Kharzeev, R. D. Pisarski, and Michel H. G. Tytgat. *Phys. Rev. Lett.*, 81:512–515, 1998.
- [3] Dmitri Kharzeev and Robert D. Pisarski. Pionic measures of parity and CP violation in high-energy nuclear collisions. *Phys. Rev. D*, 61:111901, 2000.
- [4] Kenji Fukushima, Dmitri E. Kharzeev, and Harmen J. Warringa. *Phys. Rev. D*, 78:074033, 2008.
- [5] Berndt Muller and Andreas Schafer. Charge Fluctuations from the Chiral Magnetic Effect in Nuclear Collisions. *Phys. Rev. C*, 82:057902, 2010.
- [6] Dmitri E. Kharzeev, Larry D. McLerran, and Harmen J. Warringa. *Nucl. Phys. A*, 803:227–253, 2008.
- [7] Masayuki Asakawa, Abhijit Majumder, and Berndt Muller. Electric Charge Separation in Strong Transient Magnetic Fields. *Phys. Rev. C*, 81:064912, 2010.
- [8] D. E. Kharzeev, J. Liao, S. A. Voloshin, and G. Wang. *Prog. Part. Nucl. Phys.*, 88:1–28, 2016.
- [9] Jie Zhao. *Int. J. Mod. Phys. A*, 33(13):1830010, 2018.
- [10] Jie Zhao and Fuqiang Wang. Experimental searches for the chiral magnetic effect in heavy-ion collisions. *Prog. Part. Nucl. Phys.*, 107:200–236, 2019.
- [11] B. Alver et al. System size, energy, pseudorapidity, and centrality dependence of elliptic flow. *Phys. Rev. Lett.*, 98:242302, 2007.
- [12] Sergei A. Voloshin. *Phys. Rev. C*, 70:057901, 2004.
- [13] B. I. Abelev et al. Observation of charge-dependent azimuthal correlations and possible local strong parity violation in heavy ion collisions. *Phys. Rev. C*, 81:054908, 2010.
- [14] B. I. Abelev et al. Azimuthal Charged-Particle Correlations and Possible Local Strong Parity Violation. *Phys. Rev. Lett.*, 103:251601, 2009.
- [15] L. Adamczyk et al. Beam-energy dependence of charge separation along the magnetic field in Au+Au collisions at RHIC. *Phys. Rev. Lett.*, 113:052302, 2014.
- [16] Betty Abelev et al. Charge separation relative to the reaction plane in Pb-Pb collisions at  $\sqrt{s_{NN}} = 2.76$  TeV. *Phys. Rev. Lett.*, 110(1):012301, 2013.
- [17] Vardan Khachatryan et al. Observation of charge-dependent azimuthal correlations in  $p$ -Pb collisions and its implication for the search for the chiral magnetic effect. *Phys. Rev. Lett.*, 118(12):122301, 2017.
- [18] Fuqiang Wang. *Phys. Rev. C*, 81:064902, 2010.
- [19] Adam Bzdak, Volker Koch, and Jinfeng Liao. *Phys. Rev. C*, 81:031901, 2010.
- [20] Soren Schlichting and Scott Pratt. *Phys. Rev. C*, 83:014913, 2011.
- [21] L. Adamczyk et al. *Phys. Rev. C*, 89(4):044908, 2014.
- [22] Albert M Sirunyan et al. Constraints on the chiral magnetic effect using charge-dependent azimuthal correlations in  $p$ Pb and PbPb collisions at the CERN Large Hadron Collider. *Phys. Rev. C*, 97(4):044912, 2018.
- [23] Fuqiang Wang and Jie Zhao. *Phys. Rev. C*, 95(5):051901(R), 2017.
- [24] Adam Bzdak, Volker Koch, and Jinfeng Liao. Azimuthal correlations from transverse momentum conservation and possible local parity violation. *Phys. Rev. C*, 83:014905, 2011.
- [25] Jie Zhao, Yicheng Feng, Hanlin Li, and Fuqiang Wang. HIJING can describe the anisotropy-scaled charge-dependent correlations at the BNL Relativistic Heavy Ion Collider. *Phys. Rev. C*, 101:034912, 2020.
- [26] J. Adam et al. Charge-dependent pair correlations relative to a third particle in  $p$ +Au and  $d$ +Au collisions at RHIC. *Phys. Lett. B*, 798:134975, 2019.
- [27] Jurgen Schukraft, Anthony Timmins, and Sergei A. Voloshin. *Phys. Lett. B*, 719:394–398, 2013.
- [28] K. H. Ackermann et al. STAR detector overview. *Nucl. Instrum. Meth. A*, 499:624–632, 2003.
- [29] M. Anderson et al. The Star time projection chamber: A Unique tool for studying high multiplicity events at RHIC. *Nucl. Instrum. Meth. A*, 499:659–678, 2003.
- [30] K. H. Ackermann et al. The STAR time projection chamber. *Nucl. Phys. A*, 661:681–685, 1999.
- [31] W. J. Llope. Multigap RPCs in the STAR experiment at RHIC. *Nucl. Instrum. Meth. A*, 661:S110–S113, 2012.
- [32] L. Adamczyk et al. Inclusive charged hadron elliptic flow in Au + Au collisions at  $\sqrt{s_{NN}} = 7.7 - 39$  GeV. *Phys. Rev. C*, 86:054908, 2012.
- [33] N. Borghini, P. M. Dinh, and J. Y. Ollitrault. Analysis of directed flow from elliptic flow. *Phys. Rev. C*, 66:014905, 2002.
- [34] L. Adamczyk et al. Elliptic flow of identified hadrons in Au+Au collisions at  $\sqrt{s_{NN}} = 7.7-62.4$  GeV. *Phys. Rev. C*, 88:014902, 2013.
- [35] J. Adams et al. Rho0 production and possible modification in Au+Au and p+p collisions at  $S(NN)^{1/2} = 200$ -GeV. *Phys. Rev. Lett.*, 92:092301, 2004.
- [36] Shuzhe Shi, Yin Jiang, Elias Lilleskov, and Jinfeng Liao. Anomalous Chiral Transport in Heavy Ion Collisions from Anomalous-Viscous Fluid Dynamics. *Annals Phys.*, 394:50–72, 2018.
- [37] Jie Zhao, Hanlin Li, and Fuqiang Wang. Isolating the chiral magnetic effect from backgrounds by pair invariant mass. *Eur. Phys. J. C*, 79(2):168, 2019.
- [38] Hao-Jie Xu, Jie Zhao, Xiaobao Wang, Hanlin Li, Zi-Wei Lin, Caiwan Shen, and Fuqiang Wang. Varying the chiral magnetic effect relative to flow in a single nucleus-nucleus collision. *Chin. Phys. C*, 42(8):084103, 2018.
- [39] Hanlin Li, Jie Zhao, and Fuqiang Wang. A novel invariant

mass method to isolate resonance backgrounds from the chiral magnetic effect. *Nucl. Phys. A*, 982:563–566, 2019.

[40] Gary J. Feldman and Robert D. Cousins. A Unified ap-

proach to the classical statistical analysis of small signals. *Phys. Rev. D*, 57:3873–3889, 1998.